Acta Polytechnica **65**(3):282–287, 2025
https://doi.org/10.14311/AP.2025.65.0282

Published by the Czech Technical University in Prague

COMPARISON OF CAVITATION EROSION OF NICRBSI AND AISI 316L COATINGS DEPOSITED BY POWDER PLASMA TRANSFERRED ARC WELDING

Weronika Henzler[a], Mirosław Szala[a,*], Tomasz Pałka[b], Bernard Wyględacz[c], Artur Czupryński[c], Leszek Łatka[d]

[a] *Lublin University of Technology, Faculty of Mechanical Engineering, Department of Materials Engineering, Nadbystrzycka 36D, 20-618 Lublin, Poland*

[b] *Lublin University of Technology, Faculty of Mechanical Engineering, Department of Production Engineering, Nadbystrzycka 36D, 20-618 Lublin, Poland*

[c] *Silesian University of Technology, Faculty of Mechanical Engineering, Department of Welding Engineering, Konarskiego 18A Str., 44-100 Gliwice, Poland*

[d] *Wrocław University of Science and Technology, Faculty of Mechanical Engineering, Department of Metal Forming, Welding and Metrology, Łukasiewicza St. 5, 50-371 Wroclaw, Poland*

[*] corresponding author: m.szala@pollub.pl

Abstract. This study carefully compares the effect of microstructure and hardness on the cavitation wear resistance of PPTA (Powder Plasma Transferred Arc) deposited coatings. Deposits were made on a substrate of S235JR structural steel. Two types of feedstock powder were used: material with the chemical composition of AISI 316L stainless steel, and a nickel-based, self-fluxing powder type NiCrBSi. This study involved conducting cavitation erosion tests on a vibratory test rig in accordance with the ASTM G32 standard, using the stationary specimen method. Metallographic investigations confirmed the presence of austenitic dendrites and delta ferrite precipitations in the microstructure of AISI 316L and the presence of hard carbides and borides within the nickel-based matrix of NiCrBSi hardfacing. It can be seen that the AISI 316L coating, having a much lower hardness in the range of 250–280 HV1, achieved four times poorer cavitation erosion resistance compared to the NiCrBSi coating, which has a hardness in the range of 820–890 HV1. Following the erosion testing, the AISI 316L stainless steel exhibited a mean depth of erosion of $\mathrm{MDE_{6h}} = 28.8\,\mu\mathrm{m}$, whereas the NiCrBSi hardfacing exhibited a mean depth of erosion of $\mathrm{MDE_{6h}} = 7.1\,\mu\mathrm{m}$. Moreover, NiCrBSi hardfacing exhibits a higher cavitation erosion resistance than the stainless steel coating, with erosion rates of $2.59\,\mathrm{mg\,h^{-1}}$ ($1.60\,\mu\mathrm{m\,h^{-1}}$) and $8.11\,\mathrm{mg\,h^{-1}}$ ($5.28\,\mu\mathrm{m\,h^{-1}}$), respectively. In the case of different types of overlay material, such as stainless steel and NiCrBSi coatings, the higher hardness and fine, hard particle-rich microstructure improves the cavitation erosion resistance of PPTA overlays.

Keywords: Cavitation corrosion, hardfacing, stainless steel, surface engineering, microstructure, hardness.

1. Introduction

The phenomenon of cavitation is defined as the formation and growth of bubbles in a rapidly flowing fluid due to a violent pressure drop, followed by the implosion of these bubbles when the fluid pressure increases [1, 2]. Therefore, cavitation causes severe damage to hydraulic machinery [3–5]. Cavitation erosion involves surface damage and the progressive loss of solid material due to the action of bubbles in the fluid that systematically collapse to the surface [6, 7]. It is widely accepted that the pressure and shock waves generated by the implosion of cavitation bubbles lead to material wear [8–10]. Cavitation erosion is a complex phenomenon that involves not only fluid hydrodynamic factors but also the properties of the eroded material, including its microstructure, mechanical properties, and surface morphology [11–13].

One way to protect against excessive cavitation erosion is to apply coating and protective coatings on the surface of components using welding methods [14–16]. Among the numerous surfacing methods, Powder Plasma Transferred Arc (PPTA) surfacing attracts particular attention [17, 18]. This method uses a grain size of 0.06 to 0.30 mm powder, which is melted in a plasma arc at a very high temperature. The process should be carried out at a high speed with low dilution rate to ensure high quality of the deposited coatings [19]. In addition, there is low dilution in the parent material in the overlay (can be achieved at less than 10 %) [18, 20]. Minimising the dilution helps to maintain the desired properties of the hardfacing alloy, ensuring better wear and corrosion resistance. It should also be noted that powder plasma transfer arc welding (PPTAW) is a method that has been very well adopted in the industry due to its high efficiency and relative ease of use by operators [18].

Sample determination	Type of feedstock powder (nom. chem. composition, wt. %)	Commercial name	Manufacturer	Nominal hardness
I	X5CrNiMo17-12-2 (AISI 316L)	EuTroLoy 16316	Castolin Eutectic Gliwice, Poland	~30 HRC
II	NiCrBSi (Ni – balance; 16–17 % Cr; 3.3 % B; 3.8 % Si; 0.8–1.0 % C)	Durmat 456	Durum Wear Protection GMBH Willich, Germany	56–60 HRC

TABLE 1. Filler materials (feedstock powders) used for PPTA welding and the nominal hardness of hardfacings.

Stainless steel is commonly recognised for its exceptional corrosion resistance [21, 22] and robust mechanical properties [21, 23]. However, specific applications such as those involving tribological performance show severe damage [22]. Therefore, surfacing methods such as PVD, thermal spraying, or weld overlaying prevent steel components from wear. One of the most applicable materials is nickel alloys. Nickel matrix self-fluxing alloys such as NiCrBSi alloys are promising materials that offer excellent operational properties. Mention should be made here of their resistance to abrasive wear [24], erosion [25], mechanical properties [26], and corrosion [15]. In the paper by Appiah et al. [24], the authors analysed the microstructure and performance of NiCrBSi coatings applied by PPTAW to a 15HM steel substrate. The study investigated the impact of plasma current on the microstructure, corrosion resistance, and tribological properties of materials. Of all the samples tested, the one deposited at 70 A exhibited the best overall performance, showing an optimal combination of wear resistance, corrosion resistance, hardness, and reduced grain size. It achieved a hardness measurement of 832 HV, comparable to the hardness of the surfacing analysed in the study [27] for NiCrSiBC hardfacing with an estimated average of 908 HV0.05.

Various types of metal alloys [28, 29] and composites [30, 31] are typically applied to metallic surfaces using welding methods. Most of these applications enhance abrasion resistance or help regenerate damaged components. However, only a few studies have been conducted on the cavitation resistance of NiCrBSi coatings, such as [32, 33]. Therefore, this research paper aimed to compare the influence of microstructure and hardness on the cavitation erosion resistance of nickel-based NiCrBSi with stainless steel 316L coatings surfaced by PPTAW on S235JR structural steel substrate. The comparative analysis of NiCrBSi and AISI 316L coatings, tested under cavitation conditions, both of which were deposited using the same PPTA process and tested under identical conditions, provides new valuable practical insights that are not widely reported in the current literature.

2. Materials and methods

The filler materials used to make the surfacing coatings were commercially available feedstock powders. Their characteristics and designations are shown in Table 1. The substrate material was S235JR structural steel with dimensions of $150 \times 100 \times 10$ mm, a carbon content of approximately 0.17 %, and a hardness of around 120 HV. The surfacing process used a EuTronic Gap 3511 DC Synergic (manufactured by Castolin Eutectic, Gliwice, Poland). The powder feed rates for filler materials I (X5CrNiMo17-12-2) and II (NiCrBSi) were selected as 9.68 g min^{-1} and 8.98 g min^{-1}, respectively. The other parameters remained unchanged for the process, the current was set to 100 A and the surfacing speed to 1.2 mm s^{-1}. Argon-based mixture with 5 vol. % of hydrogen (R1-ArH-5, according to the standard EN ISO 14175) was used as the shielding gas, with a flow rate of 10 slpm (standard litres per minute). The plasma and powder transport gases had a high purity of argon of 5.0, and the flow rates of the plasma and transport gases were 2 slpm and 3 slpm, respectively. The PPTA parameters were selected based on preliminary trials and previous experiments, in order to ensure proper layer quality, minimal dilution, and thick single-layer coatings (greater than 1 mm) [24, 25, 34]. Then, the fabricated overlays were machined, and their surfaces were ground and polished in preparation for investigation into further cavitation erosion.

Hardness testing and comparative tests of cavitation erosion resistance have been conducted on the polished surfaces of hardfacings, and to achieve statistical accuracy, more than 10 indentations were made. The hardness testing was performed using the FutureTech FM-700 microhardness tester in accordance with the PN-EN ISO 6507-1:2024-04 standard, which used the Vickers method for the hardness tests. The microstructure was analysed using a Phenom ProX scanning electron microscope (SEM), using the backscatter secondary electron (BSE) observation mode on the polished cross-sections of PPTA coatings.

The cavitation tests were conducted according to ASTM G32 standard requirements using an experimental setup with the stationary specimen method (Figure 1). The experiments were conducted using distilled water at a temperature of 25 ± 2 °C. The vibration frequency of the sonotrode was 20 kHz, whereas the amplitude of vibrations was 50 µm. The vibrating sonotrode was immersed in water and induced a cavitation cloud. The sonotrode tip (made of Ti6Al4V titanium alloy, with a diameter of 16 mm) was located at a standoff distance of 0.5 mm from the stationary mounted sample.

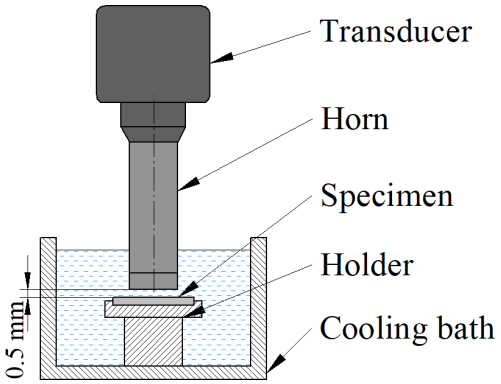

Figure 1. Cavitation erosion test rig.

For the cavitation erosion resistance tests carried out, the specimens were exposed to a vibration test rig for a specified period of time (total testing time was 6 hours), and mass loss was measured after each exposure interval to enable plotting the erosion curves. An erosion curve shows the change in material loss over a specified period.

The mass loss of the investigated material was determined with an accuracy of 0.01 mg using a precision laboratory balance. Then, the average depth of material removed from the surface due to cavitation, expressed by the mean depth of erosion (MDE), was calculated according to Equation (1). The erosion rate was calculated as the time derivative of material loss and represents the material loss per unit of time due to cavitation action.

$$\mathrm{MDE} = \frac{\text{Mass loss}}{\text{Material density} \times \text{Erosion area}} \quad [\mu\mathrm{m}]. \quad (1)$$

3. Results and Discussion

The Vickers hardness, microstructure, and erosive results are presented in Figures 2, 3 and 4, respectively. The hardness of the produced nickel-based hardfacings (Figure 2) is within the nominal hardness range quoted by the manufacturer (Table 1) and literature references [25, 35]. A broader scatter of the results was observed for the NiCrBSi sample compared to 316L, which is primarily attributed to the two-phase microstructure of 316L (Figure 3a) and the multiphase microstructure of the nickel-based hardfacing (Figure 3b). The microstructure of the NiCrBSi surfacing consists of hard carbides, borides (e.g. Cr_3C_2, $Cr_{23}C_6$, Ni_3B), and CrB embedded in a relatively soft nickel-based matrix (Figure 3) [36, 37]. This contributes to the hardness of NiCrBSi (853 HV1), which exceeds three times those reported for stainless steel. This type of microstructure provides resistance to high temperature, wear, and corrosion. The 316L sample is characterised by an austenitic structure with ferrite delta (Figure 3) [38]. A mean hardness equal to 273 HV 0.1 is consistent with the range reported for stainless steel components [39, 40]. However, it should

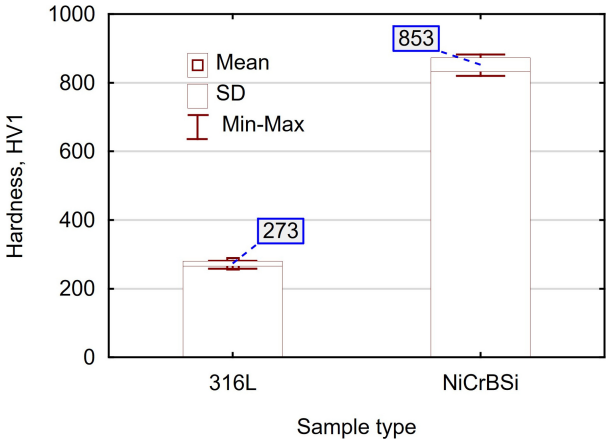

Figure 2. Microhardness of PPTAW coatings made of 316L stainless steel and NiCrBSi feedstock powders – mean value, SD (standard deviation), and scatter of measurements.

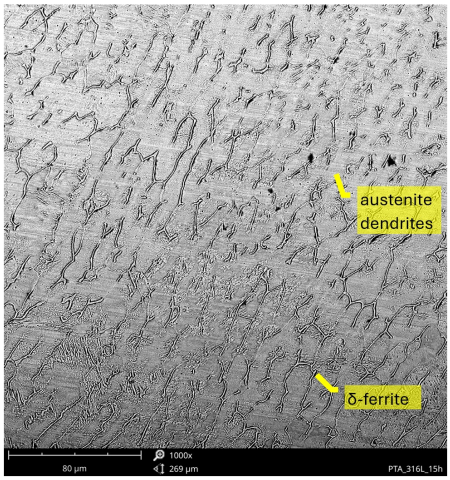

(a). Sample I (AISI 316L).

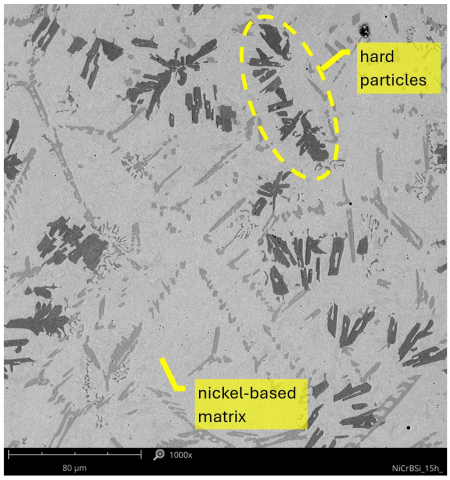

(b). Sample II (NiCrBSi).

Figure 3. The cross-section microstructure of coatings deposited by PPTA welding, SEM.

be noted that the hardness of stainless steel strongly depends on the manufacturing method, which can increase the hardness by strain hardening.

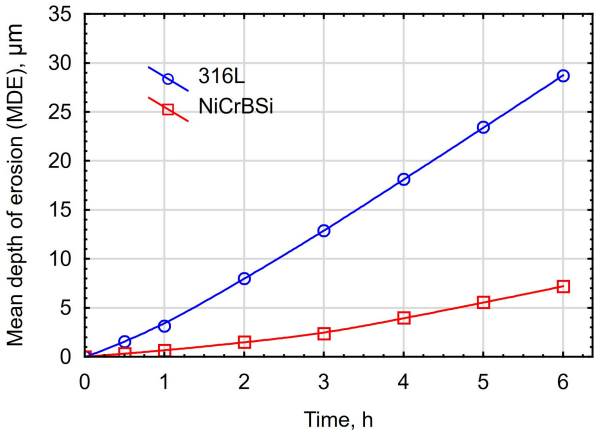

FIGURE 4. Erosion curves estimated for PPTAW overlays.

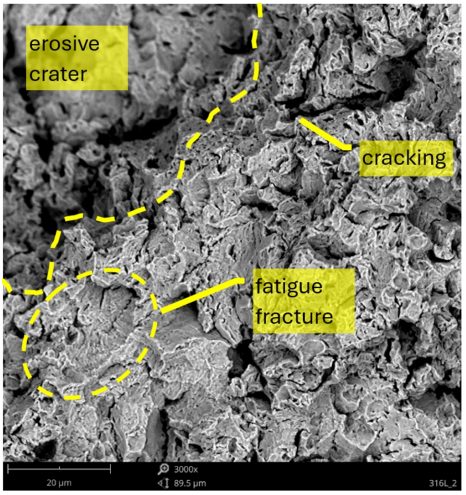

(A). Sample I (AISI 316L).

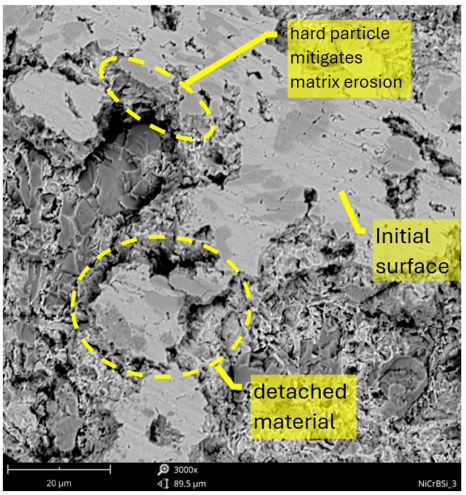

(B). Sample II (NiCrBSi).

FIGURE 5. The eroded surface of PTA overlays after three hours of cavitation erosion testing, SEM.

Cavitation erosion results indicate a higher erosion resistance for NiCrBSi than those reported for the stainless steel AISI 316L (Figure 4). Four times higher material loss, i.e. $MDE_{6h} = 28.8\,\mu m$, and higher erosion rates have been observed for 316L stainless steel samples than for NiCrBSi, i.e. $MDE_{6h} = 7.1\,\mu m$. The analysis of the cavitation erosion rates (Figure 4) and the multiphase microstructure and the high hardness of deposition II indicate that they promote cavitation resistance. Thus, NiCrBSi hardfacing shows lower erosion rates than the 316L stainless steel i.e. coating erosion rates of $2.59\,mg\,h^{-1}$ ($1.60\,\mu m\,h^{-1}$) and $8.11\,mg\,h^{-1}$ ($5.28\,\mu m\,h^{-1}$), respectively. At 6 hours of testing, the NiCrBSi hardfacing demonstrated erosion rates slightly higher than HIPed Stellites (1.88–$2.09\,mg\,h^{-1}$) [13] while showing lower rates than HVOF deposited cermet types WC-Cr3C2-Ni, WC-Co and WC-CoCr coatings ($8.61\,\mu m\,h^{-1}$, $12.76\,\mu m\,h^{-1}$ and $3.76\,\mu m\,h^{-1}$, respectively) [41] and cast ferrous metal matrix composites (6.9–$21.2\,mg\,h^{-1}$) [12]. This suggests the high potential applicability of NiCrBSi hardfacing for machine components operating in environments where cavitation erosion is a factor.

The analysis was conducted using a scanning electron microscope, allowing us to investigate the erosion mechanism and elucidate the effect of the microstructure on erosive material loss. The stainless steel surfacing was subject to uniform material removal, plastic deformation was identified, and the erosion mechanism was fatigue-like (Figure 5a), which follows the previous results [27, 42]. The erosion mechanism of the nickel deposition consisted of the selective removal of hard particles from the matrix and the formation of the crack in the eroded surface (Figure 5b). Combining the multi-phase microstructure of the nickel-based surfacing and high hardness seems beneficial in minimising erosion rates. The hard phases act as an obstacle to crack propagation, preventing material removal in large portions, and effectively increasing the erosion resistance of the hardfacings (Figure 5b). The effect of the NiCrBSi microstructure type and size of precipitation will be investigated in detail in our future works. Also, the impact of PPTA welding parameters on the cavitation erosion behaviour of PTA deposits should be analysed in the future.

4. Conclusion

This study examines the impact of microstructure and hardness on the cavitation erosion resistance of two types of hardfacing coatings: NiCrBSi and AISI 316L, both of which were applied to S235JR structural steel substrate using powder plasma transferred arc welding (PPTAW). The findings of this research lead to several key conclusions:

- The cavitation erosion tests showed that the NiCrBSi surfacing experienced approximately four times lower mass loss than the 316L surfacing; the mean depth of erosion of the NiCrBSi surfacing was approximately 7.1 µm, while for the 316L surfacing, it was more than 28.8 µm. Moreover, NiCrBSi hardfacing shows lower erosion rates, $2.59\,mg\,h^{-1}$, than AISI 316L, $8.11\,mg\,h^{-1}$.

- The effect of hardness has been investigated and observed for the studied materials. A clear difference in hardness values was observed between the two types of hardfacings: 316L (273 HV1) and NiCrBSi (853 HV1). The NiCrBSi surfacing exhibited higher hardness and resistance to cavitation erosion compared to the AISI 316L coatings.
- Metallographic investigations confirmed the austenitic dendrites and delta ferrite precipitation in the microstructure of AISI 316L and hard carbides and borides located in the nickel-based matrix of NiCrBSi hardfacing, therefore, the stainless steel surfacing eroded by removing large portions of material. However, the synergetic effect of high hardness and fine-hard particle-rich multiphase microstructure of the NiCrBSi surfacing has a beneficial impact on weakening the erosion rate of the PPTAW layers.

This preliminary study confirmed the effects of microstructure and hardness on the cavitation erosion resistance of PPTAW coatings. Moreover, NiCrBSi hardfacing has high potential applicability on machine components operating in environments where cavitation erosion is a factor. In future work, we will investigate the impact of NiCrBSi microstructure type and precipitation size in detail. Also, the effect of PPTA welding parameters on the cavitation erosion behaviour of PTA deposits should be analysed.

References

[1] J. Krawczyk, R. Jasionowski, D. Ura, et al. The effect of cavitation erosion on austenitic-ferritic steel. *Scientific Journals Maritime University of Szczecin* **56**(128):30–35, 2018. https://doi.org/10.17402/310

[2] H. Rostova, V. Voyevodin, R. Vasilenko, et al. Cavitation wear of Eurofer 97, Cr18Ni10Ti and 42HNM alloys. *Acta Polytechnica* **61**(6):762–767, 2021. https://doi.org/10.14311/AP.2021.61.0762

[3] D. E. Zakrzewska, M. H. Buszko, A. Marchewicz, A. K. Krella. Concept of cavitation erosion assessment of austenitic 1.4301 stainless steel based on roughness development. *Tribology International* **183**:108431, 2023. https://doi.org/10.1016/j.triboint.2023.108431

[4] A. K. Krella, J. Grześ, A. Erbe, M. Folstad. Behaviour of nickel coatings made by brush plating technology in conditions of cavitation erosion and corrosion. *Wear* **530–531**:204998, 2023. https://doi.org/10.1016/j.wear.2023.204998

[5] R. Jasionowski, W. Depczyński, D. Zasada. Analysis of the initial cavitation erosion period of selected nickel alloys. *IOP Conference Series: Materials Science and Engineering* **461**(1):012032, 2018. https://doi.org/10.1088/1757-899X/461/1/012032

[6] G. X. Zhou, T. Zhao, M. S. Wang, et al. Effect of main arc current on microstructure and cavitation resistance of NiCrBSi-WC alloy coating prepared by plasma transfer arc welding. *Journal of Thermal Spray Technology* **33**(8):2853–2875, 2024. https://doi.org/10.1007/s11666-024-01872-7

[7] A. Świetlicki, M. Szala, M. Walczak. Effects of shot peening and cavitation peening on properties of surface layer of metallic materials – A short review. *Materials* **15**(7):2476, 2022. https://doi.org/10.3390/ma15072476

[8] G. Gottardi, M. Tocci, L. Montesano, A. Pola. Cavitation erosion behaviour of an innovative aluminium alloy for hybrid aluminium forging. *Wear* **394–395**:1–10, 2018. https://doi.org/10.1016/j.wear.2017.10.009

[9] M. Szala, L. Łatka, M. Awtoniuk, et al. Neural modelling of APS thermal spray process parameters for optimizing the hardness, porosity and cavitation erosion resistance of Al_2O_3-13 wt. % TiO_2 coatings. *Processes* **8**(12):1544, 2020. https://doi.org/10.3390/pr8121544

[10] G. Gao, S. Guo, D. Li. A review of cavitation erosion on pumps and valves in nuclear power plants. *Materials* **17**(5):1007, 2024. https://doi.org/10.3390/ma17051007

[11] D. E. Zakrzewska, A. K. Krella. Cavitation erosion resistance influence of material properties. *Advances in Materials Science* **19**(4):18–34, 2019. https://doi.org/10.2478/adms-2019-0019

[12] Ł. Szymański, E. Olejnik, J. J. Sobczak, et al. Dry sliding, slurry abrasion and cavitation erosion of composite layers reinforced by TiC fabricated in situ in cast steel and gray cast iron. *Journal of Materials Processing Technology* **308**:117688, 2022. https://doi.org/10.1016/j.jmatprotec.2022.117688

[13] M. Szala, D. Chocyk, M. Turek. Effect of manganese ion implantation on cavitation erosion resistance of HIPed Stellite 6. *Acta Physica Polonica A* **142**(6):741, 2023. https://doi.org/10.12693/APhysPolA.142.741

[14] M. Bembenek, P. Prysyazhnyuk, T. Shihab, et al. Microstructure and wear characterization of the Fe-Mo-B-C-based hardfacing alloys deposited by flux-cored arc welding. *Materials* **15**(14):5074, 2022. https://doi.org/10.3390/ma15145074

[15] T. Zhao, S. Zhang, Z. Y. Wang, et al. Cavitation erosion/corrosion synergy and wear behaviors of nickel-based alloy coatings on 304 stainless steel prepared by cold metal transfer. *Wear* **510–511**:204510, 2022. https://doi.org/10.1016/j.wear.2022.204510

[16] M. Kaszuba, P. Widomski, P. Białucki, et al. Properties of new-generation hybrid layers combining hardfacing and nitriding dedicated to improvement in forging tools' durability. *Archives of Civil and Mechanical Engineering* **20**(3):78, 2020. https://doi.org/10.1007/s43452-020-00080-8

[17] S. BansaL, S. Kaushal, D. Gupta, V. Jain. On microstructure and cavitation erosion behavior of microwave-synthesized Ni-Al_2O_3-based composite claddings. *Surface Review and Letters* **32**(05):2240006, 2025. https://doi.org/10.1142/S0218625X22400066

[18] L. Łatka, P. Biskup. Development in PTA surface modifications – A review. *Advances in Materials Science* **20**(2):39–53, 2020. https://doi.org/10.2478/adms-2020-0009

[19] M. Bober, J. Senkara. Comparative tests of plasma-surfaced nickel layers with chromium and titanium carbides. *Welding International* **30**(2):107–111, 2016. https://doi.org/10.1080/09507116.2014.937616

[20] A. N. S. Appiah, B. Wyględacz, K. Matus, et al. Microstructure and performance of NiCrBSi coatings prepared by modulated arc currents using powder plasma transferred arc welding technology. *Applied Surface Science* **648**:159065, 2024. https://doi.org/10.1016/j.apsusc.2023.159065

[21] A. Skoczylas. Vibratory shot peening of elements cut with abrasive water jet. *Advances in Science and Technology Research Journal* **16**(2):39–49, 2022. https://doi.org/10.12913/22998624/146272

[22] M. Szala, M. Szafran, J. Matijošius, K. Drozd. Abrasive wear mechanisms of S235JR, S355J2, C45, AISI 304, and Hardox 500 steels tested using garnet, corundum and carborundum abrasives. *Advances in Science and Technology Research Journal* **17**(2):147–160, 2023. https://doi.org/10.12913/22998624/161277

[23] P. Wang, Y. Zhang, D. Yu. Microstructure and mechanical properties of pressure-quenched SS304 stainless steel. *Materials* **12**(2):290, 2019. https://doi.org/10.3390/ma12020290

[24] A. N. S. Appiah, B. Wyględacz, K. Matus, et al. Microstructure and performance of NiCrBSi coatings prepared by modulated arc currents using powder plasma transferred arc welding technology. *Applied Surface Science* **648**:159065, 2024. https://doi.org/10.1016/j.apsusc.2023.159065

[25] A. N. S. Appiah, O. Bialas, M. Żuk, et al. Hardfacing of mild steel with wear-resistant Ni-based powders containing tungsten carbide particles using powder plasma transferred arc welding technology. *Materials Science-Poland* **40**(3):42–63, 2022. https://doi.org/10.2478/msp-2022-0033

[26] M. Walczak, K. Drozd, M. Szala, J. Caban. Influence of recast NiCrMo alloy addition on porcelain-fused-to-metal bond strength. *Chiang Mai Journal of Science* **46**(4):766–777, 2019.

[27] M. Szala, M. Walczak, T. Hejwowski. Factors influencing cavitation erosion of NiCrSiB hardfacings deposited by oxy-acetylene powder welding on grey cast iron. *Advances in Science and Technology Research Journal* **15**(4):376–386, 2021. https://doi.org/10.12913/22998624/143304

[28] M. Zemlik, Ł. Konat, B. Białobrzeska. Analysis of the possibilities to increase abrasion resistance of welded joints of Hardox Extreme steel. *Tribology International* **201**:110271, 2025. https://doi.org/10.1016/j.triboint.2024.110271

[29] P. Widomski, M. Kaszuba, P. Sokołowski, et al. Nitriding of hardfaced layers as a method of improving wear resistance of hot forging tools. *Archives of Civil and Mechanical Engineering* **23**(4):241, 2023. https://doi.org/10.1007/s43452-023-00778-5

[30] P. Prysyazhnyuk, M. Bembenek, I. Drach, et al. Restoration of the impact crusher rotor using FCAW with high-manganese steel reinforced by complex carbides. *Management Systems in Production Engineering* **32**(2):294–302, 2024. https://doi.org/10.2478/mspe-2024-0028

[31] M. Bembenek, V. Tsyganov, N. Sakhniuk, et al. Tribology characteristics of heatproof alloys at a dynamic pin ladening in the variable temperature field. *Advances in Science and Technology Research Journal* **17**(5):140–152, 2023. https://doi.org/10.12913/22998624/171836

[32] M. Szala, T. Hejwowski, I. Lenart. Cavitation erosion resistance of Ni-Co based coatings. *Advances in Science and Technology Research Journal* **8**(21):36–42, 2014. https://doi.org/10.12913/22998624.1091876

[33] C. R. Will, A. R. Capra, A. G. M. Pukasiewicz, et al. Comparative study of three austenitic alloy with cobalt resistant to cavitation deposited by plasma welding. *Welding International* **26**(2):96–103, 2012. https://doi.org/10.1080/09507116.2010.527487

[34] M. Górnik, M. Lachowicz, L. Łatka. Corrosion resistance of PPTA Ni-based hardfacing layers. *Materials Science-Poland* **42**(4):66–78, 2024. https://doi.org/10.2478/msp-2024-0040

[35] A. Tahaei, B. B. Vanani, M. Abbasi, A. Arizmendi-Morquecho. The hardfacing properties of the nickel-based coating deposited by the PTA process with the addition of WC nano-particles: Wear investigation. *Tribology International* **193**:109472, 2024. https://doi.org/10.1016/j.triboint.2024.109472

[36] S. Balaguru, M. Abid, M. Gupta. Investigations on different hardfacing processes for high temperature applications of Ni-Cr-B-Si alloy hardfaced on austenitic stainless steel components. *Journal of Materials Research and Technology* **9**(5):10062–10072, 2020. https://doi.org/10.1016/j.jmrt.2020.07.010

[37] Z. Bergant, U. Trdan, J. Grum. Effect of high-temperature furnace treatment on the microstructure and corrosion behavior of NiCrBSi flame-sprayed coatings. *Corrosion Science* **88**:372–386, 2014. https://doi.org/10.1016/j.corsci.2014.07.057

[38] M. Landowski, A. Świerczyńska, G. Rogalski, D. Fydrych. Autogenous fiber laser welding of 316L austenitic and 2304 lean duplex stainless steels. *Materials* **13**(13):2930, 2020. https://doi.org/10.3390/ma13132930

[39] M. Walczak, M. Szala, W. Okuniewski. Assessment of corrosion resistance and hardness of shot peened X5CrNi18-10 steel. *Materials* **15**(24):9000, 2022. https://doi.org/10.3390/ma15249000

[40] B. Skowrońska, T. Chmielewski, M. Kulczyk, et al. Microstructural investigation of a friction-welded 316L stainless steel with ultrafine-grained structure obtained by hydrostatic extrusion. *Materials* **14**(6):1537, 2021. https://doi.org/10.3390/ma14061537

[41] E. Jonda, M. Szala, M. Sroka, et al. Investigations of cavitation erosion and wear resistance of cermet coatings manufactured by HVOF spraying. *Applied Surface Science* **608**:155071, 2023. https://doi.org/10.1016/j.apsusc.2022.155071

[42] M. Szala, L. Łatka, M. Walczak, M. Winnicki. Comparative study on the cavitation erosion and sliding wear of cold-sprayed Al/Al_2O_3 and Cu/Al_2O_3 coatings, and stainless steel, aluminium alloy, copper and brass. *Metals* **10**(7):856, 2020. https://doi.org/10.3390/met10070856